Hydrothermal synthesis and chromic properties of hexagonal WO_3 nanowires*

Yuan Hua-Jun(袁华军)†, Chen Ya-Qi(陈亚琦)†, Yu Fang(余 芳),
Peng Yue-Hua(彭跃华), He Xiong-Wu(何熊武),
Zhao Ding(赵 丁), and Tang Dong-Sheng(唐东升)‡

Key Laboratory of Low-dimensional Quantum Structures and Quantum Control of Ministry of Education, College of Physics and Information Science, Hunan Normal University, Changsha 410081, *China*

(Received 1 February 2010; revised manuscript received 23 September 2010)

This paper reports that highly purified hexagonal WO_3 nanowires are synthesized by a simple hydrothermal method. The as-synthesized WO_3 nanowires are investigated in detail by ultraviolet–visible–near infrared spectroscopy and electrical transport measurements under different conditions. It finds that the optical band gap and the diffuse reflection coefficient in the wavelength region above 450 nm of WO_3 nanowires decrease observably upon exposure to ultraviolet light or NH_3 gas. It is also found that there are electrons being trapped or released in individual WO_3 nanowires when scanning bias voltage in different directions upon exposure to ultraviolet and NH_3 gas. The experimental results suggest that the chromic properties might be attributed to the injection/extraction of hydrogen ions induced by ultraviolet light irradiation in air or creation/annihilation of oxygen vacancies induced by NH_3 gas exposure, which serve as colour centres and trap electrons as polarons. The experimental results also suggest that the hexagonal WO_3 nanowires will be a good candidate for sensing reduced gas such as NH_3.

Keywords: hydrothermal method, nanostructures, chromic property, gas adsorption
PACS: 61.46.Km, 61.72.jd, 73.23.–b, 81.07.Gf **DOI:** 10.1088/1674-1056/20/3/036103

1. Introduction

Tungsten trioxide (WO_3) films, with transparent characteristics in the visible light region owing to a large band gap of 2.5–3.5 eV, were investigated intensively because of their intriguing chromic properties and potential applications in display devices or gas sensors.[1−3] Colouration takes place when the WO_3 film is exposed to ultraviolet light (photochromism), specific gas (gaschromism) or electric field (electrochromism).[4,5] It has been proposed that oxygen vacancies serve as colour centres as there are free electrons induced by light excitation, gas adsorption or electron injection.[6,7] The WO_3 one-dimensional (1D) nanostructures, with high surface-to-volume ratio and small grain size, are expected to exhibit more outstanding photochromic, gaschromic and electrochromic properties. Recently, a number of methods, such as electrochemical techniques,[8] template directed synthesis,[9,10] solution-based colloidal approach,[11,12] chemical vapour deposition[13−15] and hydrothermal reactions,[16,17] have been developed for the preparation of WO_3 1D nanostructures. The WO_3 1D nanostructures have been shown experimentally to exhibit good sensing properties for ethanol, H_2S, NO_x, trimethylamine, and other organic compound gases.[18−21] However, there are few researches on the chromic properties of WO_3 1D nanostructures, especially on the electrochromic properties of individual WO_3 nanostructures. Furthermore, researches on the chromic properties of WO_3 1D nanostructures are necessary not only for a further understanding of the photochromism, gaschromism and electrochromism but also for the application interest.

In the present work, we synthesized highly purified diameter-monodispersed hexagonal WO_3 nanowires on a large scale by a simple hydrothermal method. The photochromic, gaschromic and electrochromic properties of the as-synthesized WO_3 nanowires were investigated in detail by ultraviolet–visible–near infrared (UV–Vis–NIR) spectroscopy. It is found that the optical band gap and the diffuse

*Project supported by the Program for New Century Excellent Talents in University (Grant No. NCET-07-0278), the Hunan Provincial Natural Science Fund of China (Grant Nos. 08JJ1001 and 07JJ6009), the Major Research plan of National Natural Science Foundation of China (Grant No. 90606010) and the Program for Excellent Talents in Hunan Normal University, China (Grant No. 070623).
†E-mail: First two authors contributed equally to this work.
‡Corresponding author. E-mail: dstang@hunnu.edu.cn
© 2011 Chinese Physical Society and IOP Publishing Ltd

reflection coefficient in the wavelength region above 450 nm of WO_3 nanowires decrease observably upon exposure to ultraviolet light or NH_3 gas. Furthermore, the chromic properties of individual WO_3 nanowires were also investigated by electrical transport measurements. It is also found that the I–V curves of individual WO_3 nanowires do not superpose themselves when bias voltage is scanned in different directions upon exposure to ultraviolet and NH_3 gas. The experimental results suggest that the chromic properties might be attributed to the injection/extraction of hydrogen ions induced by ultraviolet light irradiation in air or creation/annihilation of oxygen vacancies induced by NH_3 gas exposure, which serve as colour centres and trap electrons as polarons. The experimental results also suggest that the hexagonal WO_3 nanowires might be a good candidate for sensing reduced gas such as NH_3.

2. Experimental

All the chemicals are of analytical grade and were used without further purification. Potassium sulfate (K_2SO_4), oxalic acid ($H_2C_2O_4$), and sodium tungstate ($Na_2WO_4{\cdot}2H_2O$) were purchased from Beijing Chemical Reagent Company. In a typical experiment, sodium tungstate powder (8.15 g, 0.025 mol) was dissolved in deionized water (100 mL). The $H_2C_2O_4$ (6.3 g) was then added to the solution. After the mixture is diluted to 250 mL, a translucent, homogeneous, and stable WO_3 sol was formed. A 75 mL volume of WO_3 sol was transferred into a 100-mL autoclave, and then K_2SO_4 (3.75 g) and 6-30 drops of hydrochloric acid (HCl) were added to the sol. The autoclave was sealed and maintained at 180 °C for 48 h, and then cooled down to room temperature. The precipitates in the solution were filtered, washed sequentially with deionized water and ethanol to remove possible remnant ions, and then dried at 60 °C. The final product is the sample we have synthesized.

The sizes and morphologies of the final product were observed on a scanning electron microscope (SEM, JEOL-6360Lv). The crystal structure was determined by x-ray diffraction (XRD) (Aolong Y2000, Cu Kα, λ = 0.15405 nm). The absorption of photon was characterized by UV/Vis/NIR spectrophotometer equipped with a 60 mm integrating sphere (PerkinElmer Lambda750). In order to characterize their electrical transport properties, we first dispersed WO_3 nanowires in aqueous solution of diethylene glycol and purified them by centrifugation. Thereafter they were deposited on Au/Ti finger electrodes by putting one droplet of suspension on the surface and then baked at 180 °C for 8 hours. Electrodes were defined by using a photo-lithography technique, and formed by evapourating 15 nm AuTi on highly n-doped silicon wafer with 100 nm SiO_2 layer. Devices containing individual WO_3 nanowire were selected for electrical transport measurements. The WO_3 nanowire between two adjacent electrodes is about 700-nm long. The electrical transport measurements were carried out on a probe station in home-made sample chamber, in which the gas component can be controlled exactly by the mass flow meter.

3. Results and discussion

Typical SEM images (Fig. 1) indicate that the final product consists of highly purified nanowires without any other nanostructures such as nanobelts, nanosheets and nanoparticles. They also indicate that the as-synthesized nanowires are loosely entangled and have a uniform diameter of about 50 nm and lengths up to several tens of micrometers.

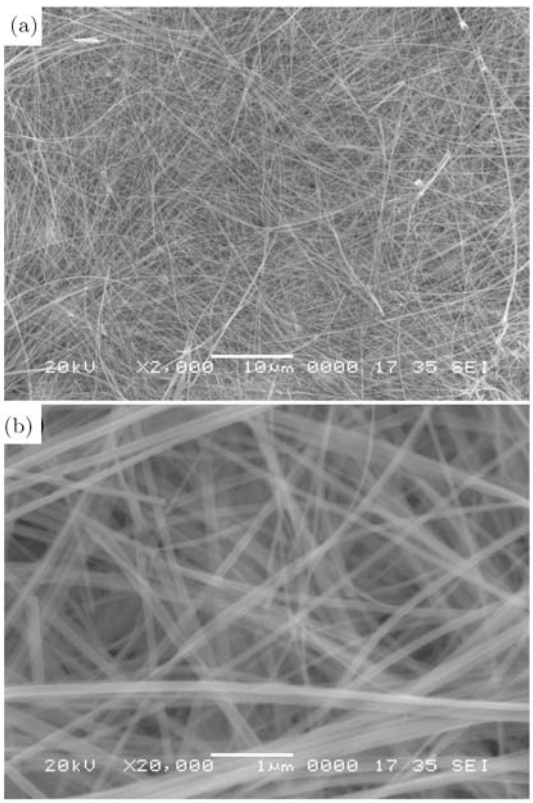


Fig. 1. Typical low-magnification (a) and high-magnification (b) SEM images of as-synthesized WO_3 nanowires. The scale bars represent 10 μm and 1 μm, respectively.

A typical XRD pattern of the as-synthesized nanowires is shown in Fig. 2. All the diffraction peaks in this pattern can be perfectly indexed as hexagonal structure of WO_3 with lattice constants of $a = b = 0.7298$ nm and $c = 0.3897$ nm (PDF card, 75-2187). It is noteworthy that no diffraction peak other than those of hexagonal WO_3 can be identified in this XRD pattern. The sharp diffraction peaks also indicate that the WO_3 nanowires are well crystallized.

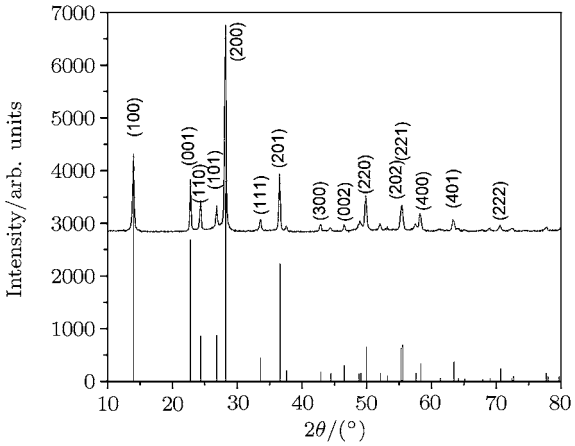


Fig. 2. The XRD pattern of the as-synthesized hexagonal WO_3 nanowires (upside) and the polycrystal diffraction spectrum of hexagonal WO_3 (PDF card, 75-2187) shown by solid lines (downside).

The WO_3 nanowires turn from light yellow to dark blue slowly when illuminated with ultraviolet light or exposed to the NH_3 gas. Figure 3(a) shows their UV/Vis/NIR diffuse reflectance spectra under different conditions, which indicates that the diffuse reflectance coefficient of WO_3 nanowires in the wavelength region above 450 nm decreases when the WO_3 nanowires are illuminated with faint ultraviolet light (365 nm, 18 W UV lamp) in air, and decreases more significantly when illuminated in NH_3 atmosphere. It also indicates a red shift in the optical absorption edge of WO_3 nanowires. In order to obtain the indirect band gap of WO_3 nanowires, the plots of $[F(R)h\nu]^{1/2}$ vs. $h\nu$ of WO_3 nanowires under different conditions are shown in Fig. 3(b). The $F(R) = (1-R)^2/2R = \alpha/S$ is the Kubelka–Munk function, where R, α and S are the diffuse reflection, absorption and scattering coefficient, respectively. The band gap of WO_3 nanowires can be defined by extrapolating the rising part of the plot of $[F(R)h\nu]^{1/2}$ vs. $h\nu$ to the photon energy axis (dotted line in Fig. 3(b)).[22] It indicates that the indirect band gap of WO_3 nanowires is about 3.09 eV, smaller than the value of 3.25 eV for bulk WO_3, which might be attributed to oxygen vacancies in the WO_3 lattice. The band gap in WO_3 is critically dependent upon bonding–antibonding interactions. Relaxation around oxygen vacancies causes increase in the W–O bond length and then decrease in the bonding–antibonding interaction, which results in a smaller band gap.[23] Figure 3(b) also indicates that the band gap of WO_3 nanowires decreases slightly to 3.04 eV when the WO_3 nanowires are illuminated about 3 hours with faint ultraviolet light in air, but decreases markedly to 2.99 eV, 2.86 eV and 2.86 eV when illuminated 1 hour, 2 hours and 3 hours in NH_3 atmosphere, respectively.

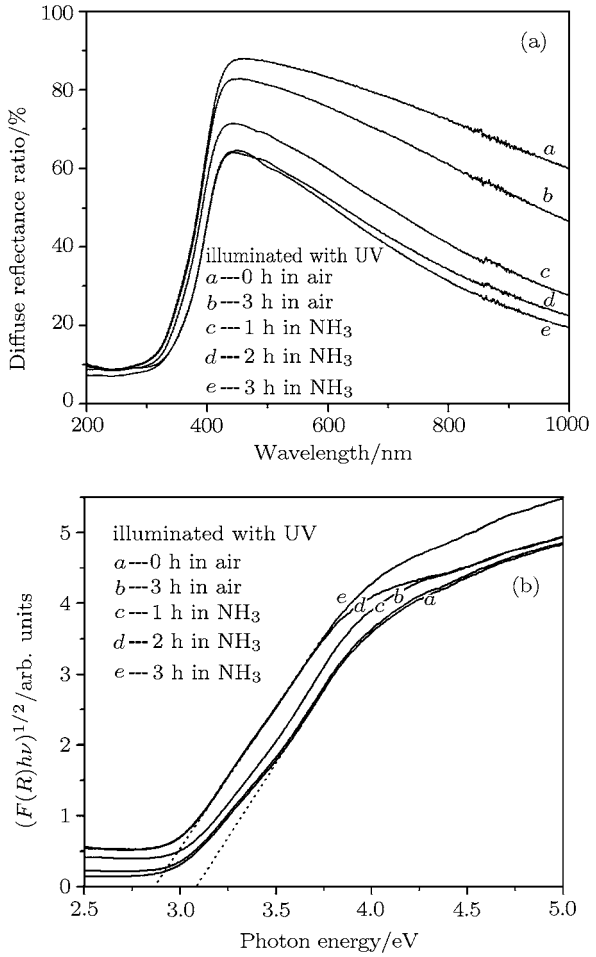


Fig. 3. The UV/Vis diffuse reflectance spectra (a) and plots of $[F(R)h\nu]^{1/2}$ vs. photon energy (b) of WO_3 nanowires when illuminated different time with faint ultraviolet light in air and NH_3 atmospheres, where R is the diffuse reflectance ratio and $F(R) = (1-R)^2/2R$ is Kubelka–Munk function.

In order to explore the photochromic, gaschromic and electrochromic reaction in WO_3 nanowires thoroughly, we also investigated the electrical transport properties of individual WO_3 nanowires illuminated

with faint ultraviolet light in different atmosphere. Figure 4 shows the atomic force microscope (AFM) image of a typical electrical device, which contains a WO_3 nanowire on top of Ti/Au finger electrodes. Current versus bias voltage (I–V_D) curves of the WO_3 nanowire under different conditions are shown in Fig. 5.

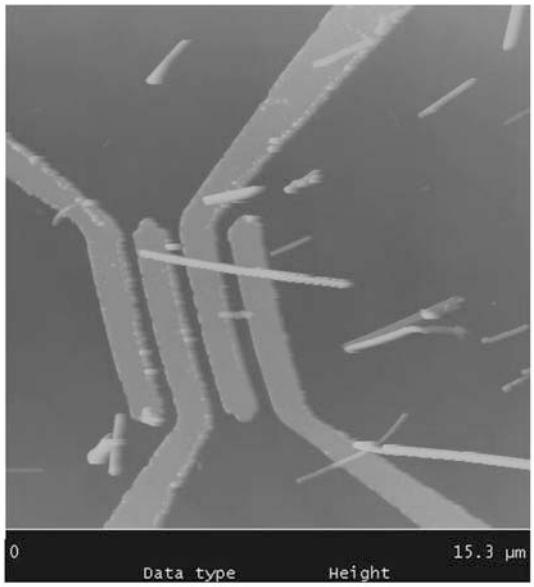


Fig. 4. The AFM image of WO_3 nanowire on top of Ti/Au finger electrodes. The WO_3 nanowire between two adjacent electrodes is about 700 nm long.

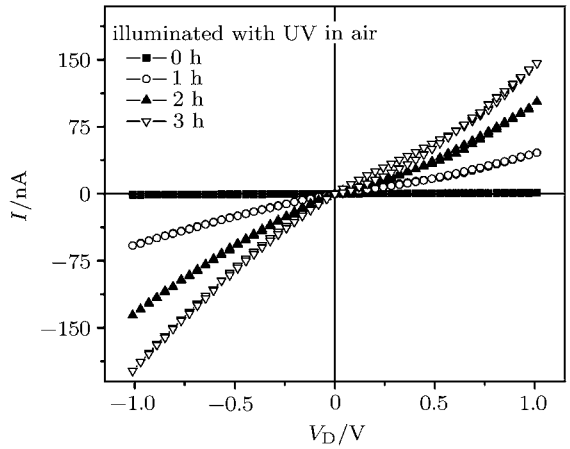


Fig. 5. The I–V_D curves of WO_3 nanowire recorded in air when illuminated with faint ultraviolet light for different times.

As shown in Fig. 6(a), the I–V_D curves are linear and symmetric in the low current region, which implies that the contacts between the WO_3 nanowire and the electrodes are of ohmic contacts. The conductance of individual WO_3 nanowires in our devices is about 1 nS under ambient conditions, which increases slowly and saturates at the magnitude of 200 nS when illuminated with faint ultraviolet light. It takes more than 2 hours for the conductance of the WO_3 nanowire to saturate, which means that the increase in conductance cannot be simply attributed to photoconduction. Furthermore, the I–V_D curves are nonlinear and asymmetric in large current region. It seems that the large current might result in Fermi-level movement in the WO_3 nanowire and then bring about asymmetric Schottky barrier in the contacts between the WO_3 nanowire and the metallic electrodes.

When the WO_3 nanowire is illuminated with 365 nm ultraviolet light, electrons near the top of its valence band can be excited to the bottom of the conduction band by absorbing photons (3.4 eV). Electron–hole pairs increase the carrier concentrations and then the conductance of the WO_3 nanowire. Moreover, there are always H_2O and O_2 molecules absorbed on the surface of WO_3 nanowire in air. Therefore, under the ultraviolet light irradiation, the possible reactions may occur on the surface of WO_3 nanowires as follows:[24]

$$\mathrm{WO_3} \xrightarrow{\mathrm{UV}} \mathrm{WO_3} + \mathrm{h^+(vb)} + \mathrm{e^-(cb)},$$
$$\mathrm{H_2O} + \mathrm{h^+(vb)} \longrightarrow \mathrm{OH}\cdot + \mathrm{H^+},$$
$$\mathrm{O_2} + \mathrm{e^-(cb)} \longrightarrow \mathrm{O_2^-}\cdot.$$

Hydrogen ions can diffuse into the lattice of WO_3nanowire and lead to the formation of HWO_3 gradually, which will result in gradual increase and saturation in the conductance of WO_3 nanowires. Therefore, the photochromic properties of WO_3 nanowires may relate to the reaction:

$$\mathrm{WO_3(transparent)} + \mathrm{H^+} + \mathrm{e^-} \longrightarrow \mathrm{HWO_3(blue)}.$$

Figure 6(a) shows that the conductance of WO_3 nanowire increases slightly when exposed to the NH_3 gas (1000 ppm). Since NH_3 is reducing gas, the increase of conductance can be attributed to the interaction of the gas with the oxygen species on the surface of the WO_3 nanowire. The possible oxidation reactions may occur on the surface of WO_3 nanowires as follows:[25]

$$2\mathrm{NH_3} + 3\mathrm{O^{2-}} \rightarrow \mathrm{N_2} + 3\mathrm{H_2O} + 6\mathrm{e^-},$$
$$2\mathrm{NH_3} + 5\mathrm{O^{2-}} \rightarrow 2\mathrm{NO} + 3\mathrm{H_2O} + 10\mathrm{e^-},$$
$$2\mathrm{NH_3} + 4\mathrm{O^{2-}} \rightarrow \mathrm{N_2O} + 3\mathrm{H_2O} + 8\mathrm{e^-}.$$

These oxidation reactions generate free electrons, which leads to the increase of the conductance of the WO_3 nanowire due to the increase of carrier concentration. On the other hand, these oxygen-consuming

reactions will also generate oxygen vacancies in the WO_3 lattice, which might answer for the decrease in the bandgap of WO_3 nanowires when illuminated with ultraviolet light in NH_3 atmosphere. As shown in Fig. 6(b), the conductance of the WO_3 nanowire increases significantly, and that the non-linearity of the I–V_D curves also decreases evidently when WO_3 nanowires are exposed to ultraviolet light. It means that the oxidation reaction rate is accelerated observably, and then the carrier density increases observably.

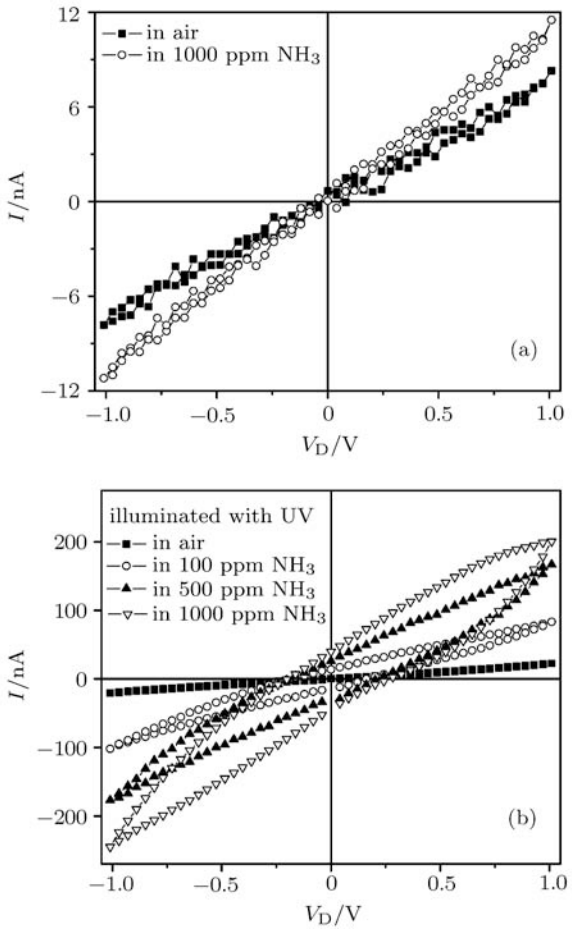


Fig. 6. The I–V_D curves of WO_3 nanowire recorded in air and NH_3 atmospheres when illuminated with daylight (a) and faint ultraviolet light (b).

The most important feature of Fig. 6(b) is that the I–V_D curves do not superpose themselves when the bias voltage is scanned in different directions, which can be named as electrical hysteresis or memory effect. Considering the red-shift of the optical absorption edge of WO_3 nanowires when illuminated with ultraviolet light in NH_3 atmosphere (Fig. 3), we suppose that the oxidation reactions on the surface do introduce a certain amount of oxygen vacancies into the WO_3 nanowire lattice, and then change their electronic structure (band gap). The oxygen vacancies might trap or release electrons slowly and then result in misalignment of I–V_D curves when the bias voltage is scanned in different directions.

When free electrons are introduced into the conduction band of WO_3 nanowires, the optical absorption of free electrons and holes may also lead to a broad absorption band extending from the near infrared to the mid-infrared. On the other hand they might be captured by oxygen vacancies, or move around oxygen vacancies in a spatially localized level accompanied by a local deformation in the lattice, which will affect the electronic environment of the neighbouring tungsten ions and reduce their valences from +6 to +5 or +4 partially. The electrons can hop from a W^{5+} site to a neighbouring W^{6+} site by absorption of photon energy,[26] which will cause a broad absorption band extending from 450 nm to the near infrared, resulting in the bluish appearance of the WO_3 nanowires. The oxygen vacancies might trap or release electrons slowly and then result in misalignment of I–V_D curves when the bias voltage is scanned in different directions. Therefore, the misaligned I–V_D curves scanned in different directions might correspond to the process of colouration/bleaching of the WO_3 nanowires.

According to previous reports,[27−29] the colouration/bleaching of WO_3 film is directly related to the double injection/extraction of positive ions and electrons or creation/annihilation of oxygen vacancies. However, in our case, the chromic properties of WO_3 nanowires are ascribed to the double injection/extraction of hydrogen ions and electrons when illuminated with ultraviolet light in air, and to creation/annihilation of oxygen vacancies when exposed to NH_3 atmosphere.

4. Conclusion

We have successfully synthesized highly purified diameter-monodispersed hexagonal WO_3 nanowires on a large scale by a simple hydrothermal method. The chromic properties of the as-synthesized WO_3 nanowires are investigated in detail by UV–Vis–NIR spectroscopy and electrical transport measurements. It is found that the optical band gap and the diffuse reflection coefficient in the wavelength region above 450 nm of WO_3 nanowires decrease observably upon exposure to ultraviolet light or NH_3 gas. It is also found that the I–V curves of individual WO_3 nanowires

do not not superpose themselves when the bias voltage is scanned in different directions upon exposure to ultraviolet light and NH_3 gas. The experimental results suggest that the chromic properties might be attributed to the injection/extraction of hydrogen ions induced by ultraviolet light irradiation or creation/annihilation of oxygen vacancies induced by NH_3 gas exposure, which serve as colour centres and trap electrons as polarons. The experimental results also suggest that the hexagonal WO_3 nanowires will be a good candidate for sensing reduced gas such as NH_3 at room temperature.

References

[1] Turyan I, Krasovec U O, Orel B, Saraidorov T, Reisfeld R and Mandler D 2000 *Adv. Mater.* **12** 330
[2] Granqvist C G 2000 *Sol. Energy Mater. Sol. Cells* **60** 201
[3] Jelle B P and Hagen G 1999 *Sol. Energy Mater. Sol. Cells* **58** 277
[4] Avellaneda C O and Bulhoes L O S 2003 *Solid State Ionics* **165** 117
[5] Gavrilyuk A I 1999 *Electrochim. Acta* **44** 3027
[6] Deb S K 1973 *Philos. Mag.* **27** 810
[7] Granqvist C G 1993 *Appl. Phys.* A: *Solid Surf.* **57** 3
[8] Gu G, Zheng B, Han W Q, Roth S and Liu J 2002 *Nano Lett.* **2** 849
[9] Lakshmi B B, Dorhout P K and Martin C R 1997 *Chem. Mater.* **9** 857
[10] Satishkumar B C, Govindaraj A, Nath M and Rao C N R 2000 *J. Mater. Chem.* **10** 2115
[11] Lee K, Seo W S and Park J T 2003 *J. Am. Chem. Soc.* **125** 3408
[12] Hudson M J, Peckett J W and Harris F 2003 *J. Mater. Chem.* **13** 445
[13] Liu Z W, Bando Y and Tang C C 2003 *Chem. Phys. Lett.* **372** 179
[14] Klinke C, Hannon J B, Gignac L, Reuter K and Avouris P 2005 *J. Phys. Chem.* B **109** 17787
[15] York A P E, Sloan J and Green M L H 1999 *Chem. Commun.* **3** 269
[16] Li X L, Liu J F and Li Y D 2003 *Inorg. Chem.* **42** 921
[17] Lou X W and Zeng H C 2003 *Inorg. Chem.* **42** 6169
[18] Solis J L, Hoel A, Kish L B, Sauko S and Granqvist C G 2000 *J. Am. Ceram. Soc.* **84** 1504
[19] Chen H J, Xu N S, Deng S Z, Lu D Y, Li Z L, Zhou J and Chen J 2007 *Nanotechnology* **18** 205701
[20] Satnkova M, Vilanova X, Llobet E, Calderer J, Bittencourt C, Pireaux J J and Correig X 2005 *Sens. Actuators* B **105** 271
[21] Xu Y X, Tang Z L, Zhang Z T, Ji Y M and Zhou Z G 2008 *Sens. Lett.* **6** 1
[22] Smith W, Zhang Z Y and Zhao Y P 2007 *J. Vac. Sci. Technol.* B **25** 1875
[23] Chatten R, Chadwick A V, Rougier A and Lindan P J D 2005 *J. Phys. Chem.* B **109** 3146
[24] Zhang M, Chen C C, Ma W H and Zhao J C 2008 *Angew. Chem. Int. Ed.* **47** 9730
[25] Jimenez I, Centeno M A, Scotti R, Morazzoni F, Arbiol J, Cornet A and Morante J R 2004 *J. Mater. Chem.* **14** 2412
[26] Schirmer O F, Wittwer V, Baur G and Brandt G 1977 *J. Electrochem. Soc.* **124** 749
[27] Granqvist C G 2000 *Sol. Energy Mater. Sol. Cells* **60** 201
[28] Georg A, Graf W, Neumann R and Wittwer V 2000 *Solid State Ion.* **127** 319
[29] Faughnan B W, Crandall R S and Heyman P M 1975 *RCA Rev.* **36** 177